INTERNATIONAL JOURNAL OF AUTOMOTIVE AND MECHANICAL ENGINEERING (IJAME)
ISSN: 2229-8649 e-ISSN: 2180-1606
VOL. 18, ISSUE 1, 8577 – 8584
DOI: https://doi.org/10.15282/ijame.18.1.2021.16.0651

ORIGINAL ARTICLE

The Magnetorheological Fluid: Testing on Automotive Braking System

A.Z. Zainordin[1*], Z. Mohamed[2] and F. Ahmad[3]

[1,2]Advanced Structural Integrity and Vibration Research Group (ASIVR), Fakulti Teknologi Kejuruteraan Mekanikal dan Automotif, Universiti Malaysia Pahang, 26600 Pekan, Pahang, Malaysia
[3]I-Mobility Research Group, Centre for Advanced Research on Energy (Cares), Faculty of Mechanical Engineering, Universiti Teknikal Malaysia Melaka, 75450 Ayer Keroh, Melaka, Malaysia

ABSTRACT – This paper presents testing of the magnetorheological brake (MRB) in the braking system of a vehicle. Two techniques are used to determine the capability of the brake system, which are simulation via Matlab Simulink Software and experimental study by using a quarter vehicle test rig. A Proportional-Integral-Derivative (PID) is employed as a wheel speed control and enforces the MRB to produce the required braking torque need by a vehicle. A dynamic test, namely sudden braking test, is performed in three rotational speed conditions, which are from 127.5 rad/s (1200 rpm) to 31.42 rad/s (300 rpm), 52.37 Rad/s (500 rpm) and 73.31 rad/s (700 rpm) in two different wheel load which are 10 kg and 15 kg, respectively. The behaviours to be assessed are wheel speed response and brake torque produced by the MRB. From the observation, the MRB's capability in providing the required brake torque is promising and harmony between simulation and experimental response.

ARTICLE HISTORY
Received: 17th Mar 2020
Revised: 9th Mar 2021
Accepted: 17th Mar 2021

KEYWORDS
Magnetorheological brake; Magnetorheological fluid; Sudden braking test; Wheel speed control

INTRODUCTION

Strong technology development gradually increased the presence of electronics in the engineering industry, especially in motor vehicle. The use of electrical and electronic components in vehicles had improved motor vehicle performance with a significant reduction in production cost and an increase in both active and passive safety. Furthermore, electronic technology facilitates introducing a new function that would be costly or not even workable by using a mechanical or hydraulic system alone. This new technological development formerly confines to features such as motor control, wiper, light, or door control, which now has affected all car domains even for the critical function. This trend generally begins with the x-by-wire concept, whereby mechanical or hydraulic systems embedded in the automotive application will be replaced by fully electric or electronic. One of the best examples of using x-by-wire in a vehicle is the brake-by-wire (BBW) system.

The concept of the BBW is motivated by the enforcement of stringent active safety standard of the automotive society that needs an active braking system in a vehicle. The active braking system, known as the Advanced Emergency Braking System, has used a vehicle sensor and has required a fast response actuate to react effectively during a critical situation [1]. However, fulfilling this requirement with conventional hydraulic braking (CHB) system has been difficult due to its limitations, such as delay response time up to 300 ms and the hysteresis characteristic of the hydraulic fluid [1]. Furthermore, the two-step control of a hydraulic valve in the CHB system is the major drawback of the brake system, thus preventing the active control technology from being implemented.

As a solution to the drawback of the CHB, many new braking systems have been invented, such as electro-hydraulic brake (EHB) [2–4], electro-pneumatic brake (EPB) [5–7] and an electromechanical brake (EMB) [8–10]. However, the most accurate description of BBW is the EMB because the brake fluid and hydraulic lines are eliminated. Since it had been introduced in 1989, many patents have been claimed in different design of EMB [11–16]. In those inventions, four common features have been identified in all designs. Most of the EMBs consists of an electric motor drive, some reduction gear, a floating disc brake calliper type and used 24/42-volt power supply [11–16]. However, the power requirement cannot be fulfilled by using the internal battery of a normal vehicle due to the existing vehicles use a 12V power supply only [12][17]. Concurrently, with the extensive investigation of the EMB, automotive engineers try to search for other techniques to take advantage of EMB. Therefore, the EMB based magnetorheological fluid (MRF) known as a magnetorheological brake (MRB) has appeared to be one of the most interesting models to be investigated. MRB employs MRF that has been immersed between the gaps of a disk enclosure in a static casing to produce a brake torque. MRF is a class of intelligent material that forms a chain-like structure when exposed to an external magnetic field, thus produce a shear force that turns into braking torque to the vehicle.

To date, many types of research on MRB have been conducted. Nam and Ahn have proposed a higher resistance of a rotary disk with waveform boundary and has provided more resistance torque when compared to conventional MRB [18]. Meanwhile, Nguyen and Choi have carried out an optimal design of MRB for a middle-sized motorcycle by considering temperature effects while the braking process concerning the mass and brake size [19]. On the other hand, Sohn et al.

***CORRESPONDING AUTHOR** | Ahmad Zaifazlin Zainordin | zaifazlin123@gmail.com

have performed a study of MRB torque characteristic between conventional and has modified magnetic core shape via evaluation experiment [20]. Moreover, George et al. have explored the potential of MRB for all-terrain vehicles by optimising the braking parameter via finite element analysis [21]. Meanwhile, Shiao et al. have proposed a new design of MRB by proposing multiple electromagnetic poles to improve brake torque [22], and Qin et al. have carried out a small-scale multi-drum design of MRB as a haptic device and have evaluated the performance through experiment [23]. Although studies on this matter have shown several improvements, a thorough study of the system is still lacking and have some limitations. The studies by previous researchers mainly focused on the model characterisation, but little attention is paid to the control and testing of the MRB. Some successful control and implementation have been recorded using quarter cars test rig such as [12, 17, 24–26] and an actual vehicle [26][27]. However, the experiment results have shown some delay in response signal and not concur with relating theories due to the malfunction of the system and the safety issues [24, 26, 27].

In this study, as an effort to contribute to the progression in the BBW, testing of MRB in halting a wheel is investigated. To access the compatibility between theory or simulation, the evaluation has been made by comparing the wheel speed and brake torque response between simulation and experiment. Noted that the MRB design, the test rig, as well as the characterisation of the brake design that has been used in this study, can be found in [28] and [29]. The outline of this paper has been arranged as follows; the first section introduces MR fluid in the vehicle brake system. Then, Section 2 presents the explanation of the model and hardware for MRB testing followed, by section 3, which presents the testing equipment. Next, section 4 presents the control strategy of MRB. After that, section 5 presents the testing procedure of MRB with the discussion of the results obtains. Finally, the conclusion of the works is presented in Section 6.

MODELS AND HARDWARE FOR MAGNETORHEOLOGICAL BRAKE TESTING

To determine the capability of the MRB in a wheel decelerating, a validate wheel dynamic model with MR fluid type 132-AD [30] that have been used is shown in Figure 1. As illustrated, it consists of a drive shaft that connects to the three-phase motor through belting that provides a throttle torque, an MRB that provides the brake torque and a steel load that represents a dynamic wheel. The MRB consists of three parts that are a moving rotor, a static body and a winding coil. Moving rotor and a static body are made from mild steel and a winding coil that has been used in this design are made from bronze wire [31]. Meanwhile, a connection between MRB and a drive shaft that consists of the moving rotor is linked to the drive shaft via jaw coupling.

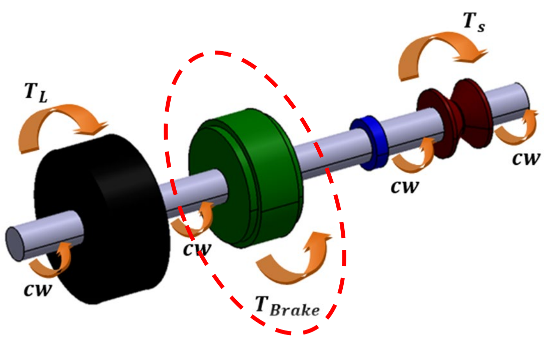

Figure 1. Dynamic motion of MR brake.

Referring to Figure 1, the equation of motion of the system is described as:

$$T_s - T_{brake} - T_c = J_{all}\alpha \tag{1}$$

where, T_{brake} is the brake torque, T_c is the bearing viscous damping, T_s is the drive torque while the shaft is rotating and J_{all} is the total inertia. Since the rotation of the drive shaft is initiated by the motor torque, T_m and amplified by the load torque, T_L that has a weight m rotating within the effective radius r_L, the T_s can be rewritten as:

$$T_s = T_m + T_L \tag{2}$$

where,

$$T_m = \left(\frac{P_m}{\omega_m}\right) \tag{3}$$

and

$$T_L = mgr_L \tag{4}$$

Noted that P_m, ω_m, and g is the power of the electric motor, electric motor angular velocity and gravitational velocity, respectively. On the other hand, T_{brake} is the brake torque that is generated by shear friction between the static and moving parts of MRB. Two main components that are contributed to the generation of braking torques are the torque due to the effect of the magnetic field (T_H) and the torque due to the viscosity of fluid (T_μ). Mathematically, it can be expressed as:

$$T_{brake} = T_H + T_\mu \tag{5}$$

Where

$$T_H = \frac{2\pi}{3} NkH^\beta \alpha_i ({r_o}^3 - {r_i}^3) i \tag{6}$$

and

$$T_\mu = \frac{\pi}{2h} N\mu_p ({r_o}^4 - {r_i}^4)\omega_s \tag{7}$$

where N is the rotor surface numbers, r_i and r_o are the inner and outer radius, ω_s is the rotor angular velocity and the brake rotor outer radius. Meanwhile, H^β is the magnetic field intensity, i is the current that is applied to the magnetic coil, while α_i, k and β are the MR fluid constant parameters, respectively.

Otherwise, since the total moment of inertia (J_{all}) consists of a rotor, a shaft, a four pillow bearing, a sprocket wheel, a V-type pulley and a steel load; the equation is written as $J_{all}\alpha = ((P_m/w_m) + mgr_L) - (T_H + T_\mu) - 4cw$. Upon calculation, the J_{all} values are 0.35 kg.m^2 and 0.454 kg.m^2 when 10 kg and 15 kg steel loads are added to the system, respectively. The technical specification details of the system are listed in Table 1.

Table 1. MR brake model parameters.

No.	Symbol	Description	Value
1.	μ_p	Fluid viscosity	0.1-1 Pa.s
2.	N	Number of surfaces	2
3.	h	Fluid gap	0.0025 m
4.	α_i	Proportional gain	12500 m^{-1}
5.	r_o	The outer rotor radius	0.04 m
6.	r_i	The inner rotor radius	0.01 m
7.	r_L	The outer radius of load	0.09 m
8.	c	Constant viscous damping	0.08

HARDWARE AND TESTING APPARATUS

In this experiment, the capability of the MRB is determined by using the same test rig that has been used in [31] as shown in Figure 2. It consists of an electric motor to actuate a drive shaft via an A-type V-belt, load cells that have been coupled with a 238 mm arm to sense a brake torque that is produced by MRB and a wheel speed sensor to sense an angular velocity of a drive shaft. An Integrated Measurement and Control (IMC) are used as the input/output devices for signal processing.

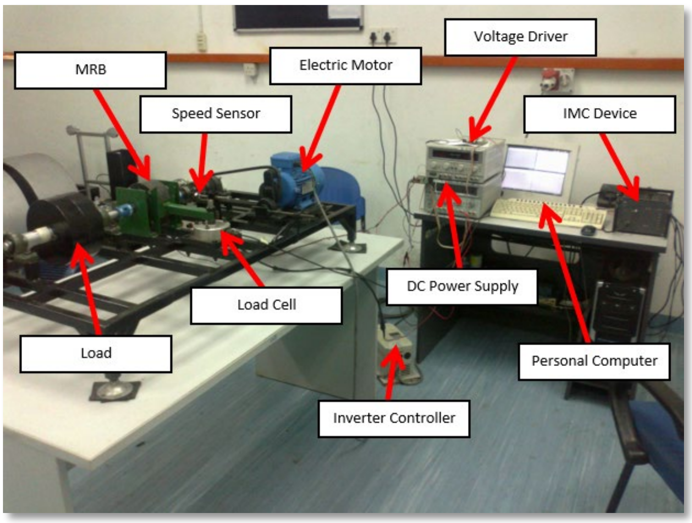

Figure 2. Mechanical assembly of the MR brake test rig.

THE CONTROL STRATEGY OF MR BRAKE

Figure 3 shows the MRB control strategy. It consists of one main controller loop known as wheel speed control that governs the overall output of the wheel dynamic by using a proportional–integral– derivative (PID) controller. The braking ability of the MRB is influenced by a wheel velocity (ω_s), and an actual wheel angular velocity (ω_a) is fed back to the MRB actuator. In this experiment, the controller parameters are tuned by the method of trial and error, which later is verified through sensitivity analysis. Analysis results show that the optimum parameter for proportional gain, $K_p(t)$, integral gain, $K_{\mathrm{i}}(t)$ and derivative gain, $K_{\mathrm{d}}(t)$ are 44, 0.001 and 0.03, respectively.

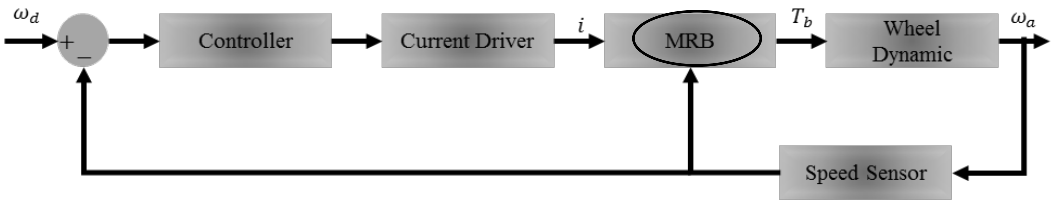

Figure 3. MRB control strategy.

The MRB model needs to be verified with the experiment in order to study the wheel angular velocity and braking torque responses. Based on the numerical model that has been developed by [28], the responses of wheel angular velocity and braking torque are similar to this experiment. In addition, the MRB torque proportionally increases when the current increases and independent of the rotational speed. The MRB model is developed by following the behaviour trend of MRB that is gathered through experiment. The MR brake actuator model is developed based on the characteristics of the MR brake, where the brake torque increases proportionally with apply current and independent speed [30],[31],[32]. In this model, the actuator is designed based on rotational wheel speed, and it is assumed that the torque remains the same at all speed.

The simulation and experimental techniques that have been used in this study are based on the techniques that have been used in [28], whereby a quarter vehicle model is able to produce speed 200 rpm to 1200 rpm. The shifting idea is stated below:

$$\text{If} \quad w_a \leq w_d, \qquad T_b = \text{brake off} \tag{8}$$

$$\text{Else} \quad w_a > w_d, \qquad T_b = \text{brake on} \tag{9}$$

The shifting equation stated above is used in the simulation of the MRB model in MATLAB based on an actual MRB characteristic, as shown in Figure 4. It is known that the torque responses generated by a brake are depended on wheel angular velocity. This model is used to verify the controllable wheel speed results obtained in this experiment with the brake torque simultaneously. The brake torque is supplied continuously to maintain the desired speed (w_d) thus providing enough braking to keep the wheel speed at a certain speed. As stated in Eq. (8) and (9), when the wheel speed is less than or equal to desired wheel speed, brake torque is not produced by the MRB. If an actual speed is greater than the desired speed, an error occurred. The error that occurred is corrected by a controller by continuously supplying the current to MRB until the desired speed is reached. Based on the proposed technique, the braking torque at a constant steady-state can be achieved. By referring to Figure 4, the MRB actuator model consists of 6 blocks, which represents the brake model based on an actual characteristic of MRB obtained from the experiment in Zainordin et al. [30]. Each block is connected to the shifting block as a function torque selector depending on the wheel angular velocity by referring to Eq. (8) and (9). The block is designed from 200 rpm to 1200 rpm with a step increment of 200 rpm for each block. A current is applied to the current driver to activate the MRB until the wheel speed reached the desired speed. The times took to reach the steady-state depending on the load that is attached to the system. Previous researchers have used the same model to study the angular speed, torque and stopping distance via a comparison between simulation and experiment [28].

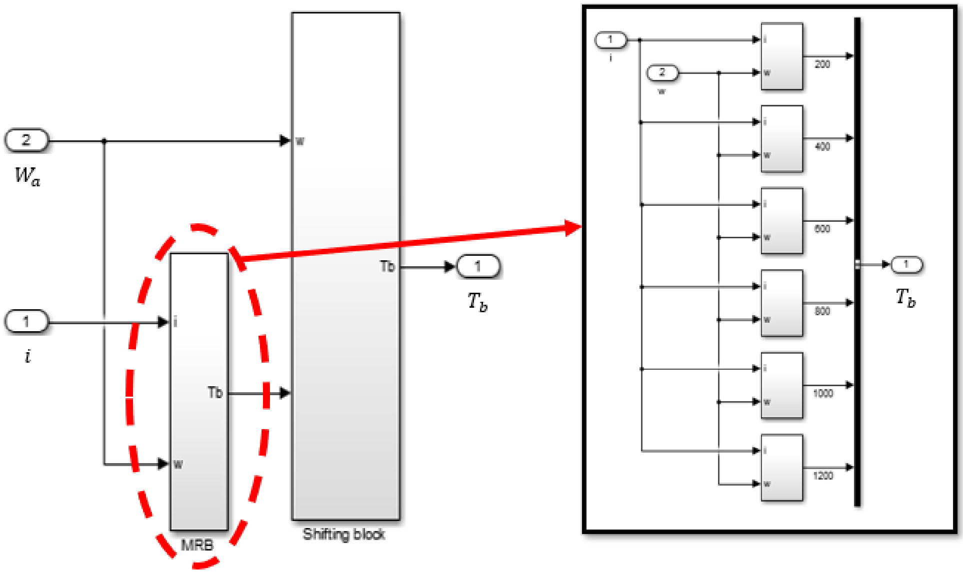

Figure 4. MRB actuator model with shifting block.

RESULTS AND DISCUSSION

The main purpose of this assessment is to inspect the capability and the potential benefit of the proposed MRB actuator in providing a braking response to slow down a wheel. This method is to make the braking severe enough to cause the steel wheel load to slow down according to the desired speed need by a driver. Furthermore, it is an attempt to represent a critical braking situation where the highest performance of the braking system is adequately challenged. This test intended to show braking ability which may play a major role in preventing an accident. By using the stated brake test rig, handling test procedure, namely sudden braking test, is carried out. In this stage, the assessments were performed in three rotational speed conditions, which are from 127.5 rad/s (1200 rpm) to 31.42 rad/s (300 rpm), 52.37 rad/s (500 rpm) and 73.31 rad/s (700 rpm), which used two different loads of 10 kg and 15 kg, respectively. The simulations and experiment results of the braking test at all loads and speed conditions are shown in Figure 5 and Figure 6.

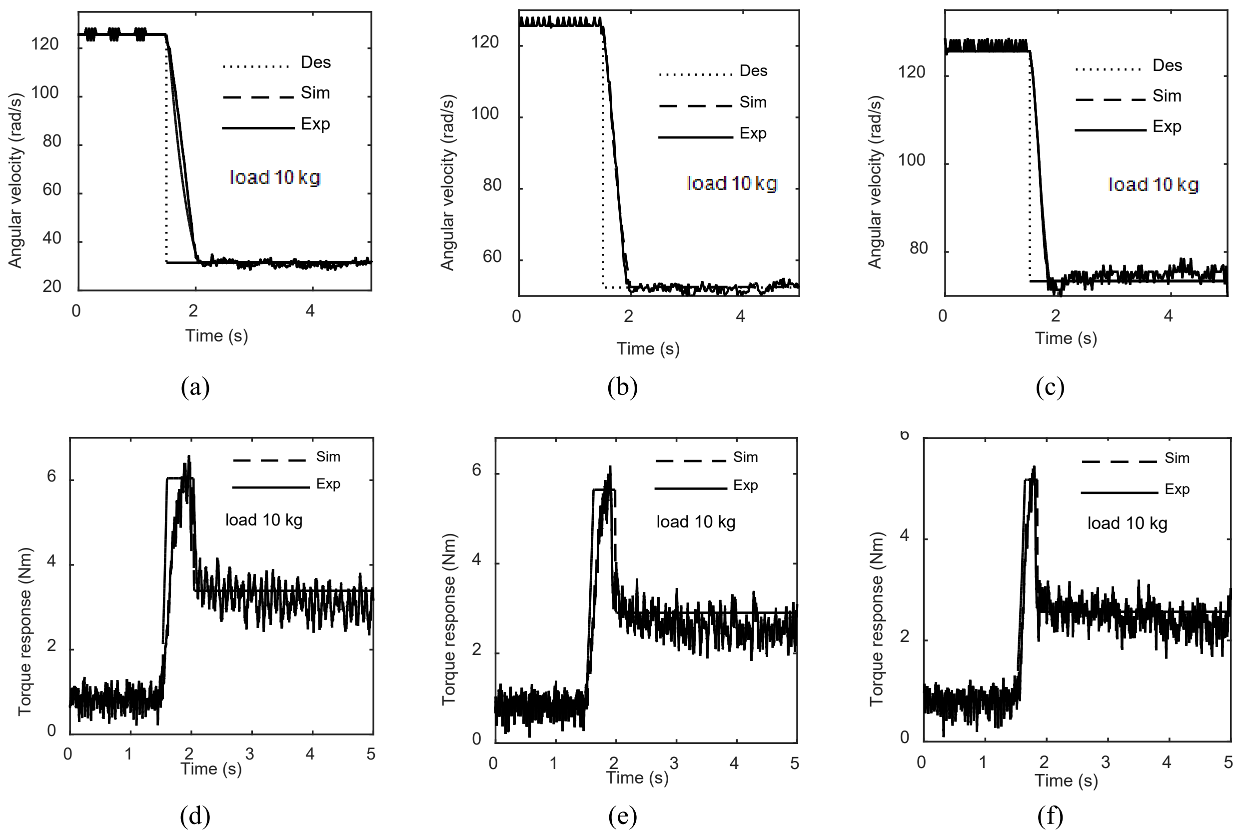

Figure 5. Responses of wheel braking using MRB at 10 kg load and rotational speed of (a), (d) 127.5 to 31.42 rad/s, (b), (e) 127.5 to 52.37 rad/s, and (c), (d) 127.5 to 73.31 rad/s.

In this study, the observation is made by examining two main behaviours of the wheel dynamic, namely wheel speed and brake torque responses, that are provided by the MRB system. The investigation of the wheel speed responses aimed to see the data compatibility between the model and the hardware, thus validating the simulation model. From the investigation, the behaviour of the simulation model, together with the appropriate brake controller, is almost similar to the behaviour of the hardware. However, there is a small difference occurring in the transient responses, especially when the system reaches and saturate at the desired speed. The difference in the results is due to the fact that it is difficult for the hardware to maintain the constant ideal speed during braking due to the inertia of the wheel. The mismatched data between simulations and experiment are recorded in Table 2. The data shows that the error between these responses is almost less than 5 % error. According to Hudha [33], the essential characteristics in the control-oriented model is the trend of the model responses. As long as the trend of the model responses is closely similar to the measure responses with an acceptable level of deviations and errors, the results are acceptable. Aside from that, Rykiel [34] mentioned that the satisfaction level of deviation between measure and simulate responses are below than 5 % of error. Therefore, based on the statement, the model is realistic and can be used as the basis for assessing the effectiveness of the proposed MRB.

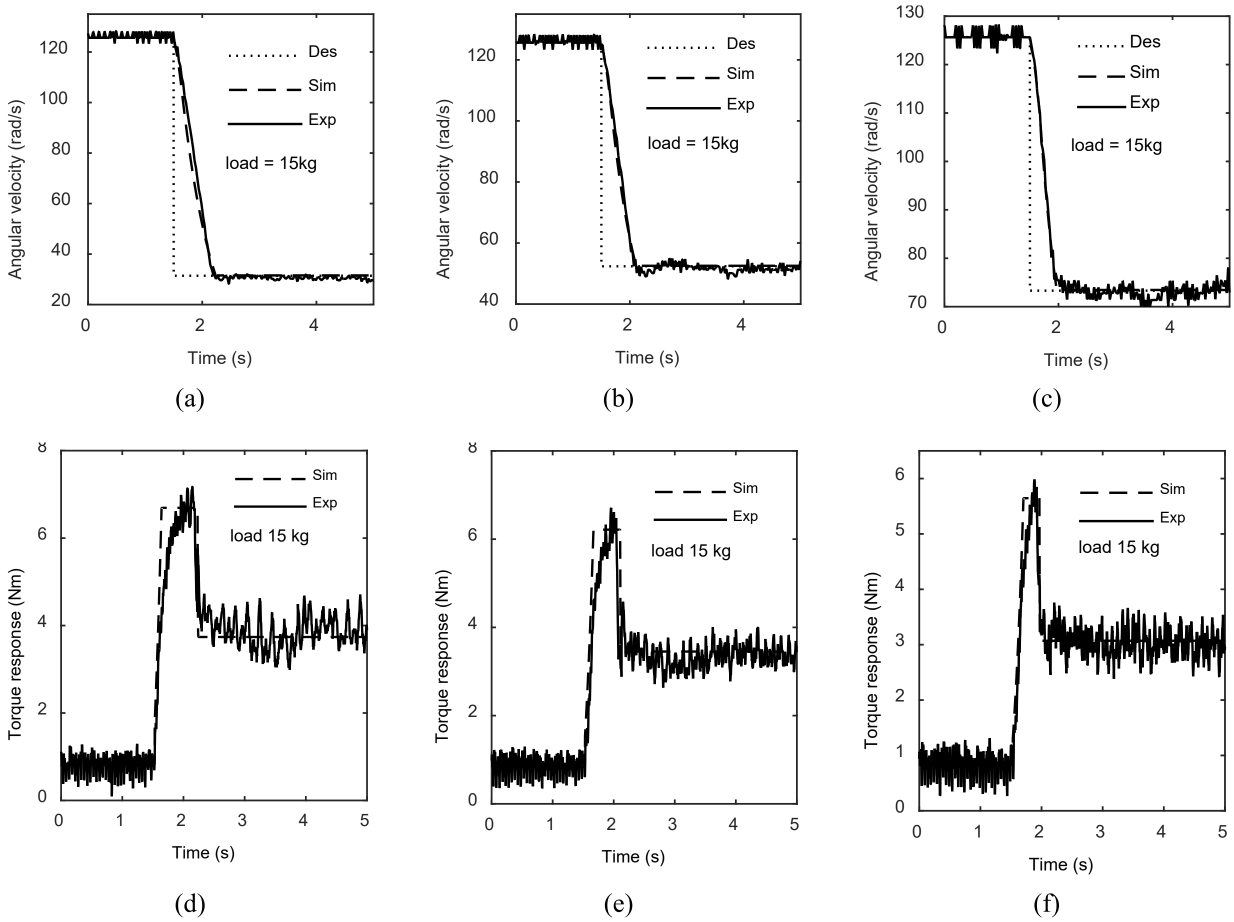

Figure 6. Responses of wheel braking using MRB at 15 kg load and rotational speed of (a), (d) 127.5 to 31.42 rad/s, (b), (e) 127.5 to 52.37 rad/s, and (c), (f) 127.5 to 73.31 rad/s.

In addition, the differences between the results are contributed by the slow braking torque delivered by the MRB hardware system. It is clearly shown in the torque responses figure that even though the wheel speed responses are almost similar, the ability of the MRB hardware to reach the necessary braking torque is 0.25 second slower than the simulations. This difference is due to the internal friction within the hardware system, especially between two unsmooth contact surfaces and the inertia of the internal components of the MRB that has caused the slow responses in the experimental system. Moreover, the mismatch in the torque responses between the simulations and the experiment is also contributed by the performance of the force sensor, where the sensitivity of the sensor is unable to capture the smallest torque produce by the MRB. This is due to the existence of clearance at the connection between the load cell sensor and the arm that has degraded the response of the MRB hardware. The difference between simulations and experiment are recorded in Table 2 and 3, whereby the percentage of deviation between simulations and experiment is almost less than 6 %.

Table 2. RMS values and deviation percentage of the shaft angular velocity.

Angular speed (rad/s)	RMS shaft angular velocity response (rad/s)					
	10 kg			15 kg		
	Simulation	Experiment	Deviation error (%)	Simulation	Experiment	Deviation error (%)
31.42	31.57	31.93	1.14	30.56	29.67	2.91
52.37	52.52	52.31	0.4	52.54	53.68	2.17
73.31	73.48	70.05	4.67	73.46	72.92	0.74

Table 3. RMS values and deviation percentage of torque response

Angular speed (rad/s)	RMS torque response (N)					
	10 kg			15 kg		
	Simulation	Experiment	Deviation error (%)	Simulation	Experiment	Deviation error (%)
31.42	3.386	3.184	5.97	3.738	3.896	4.22
52.37	2.903	3.071	5.79	3.452	3.567	3.33
73.31	2.668	2.829	6.03	3.070	2.955	3.75

The results show that the efficacy of PID control is undeniable. It acts well to produce the required braking torque either in simulation or experiment. The efficacy is due to the effectiveness of the controller nature that is able to provide excellent control performance despite variation in the dynamic characteristics of a process plant beside easy to be tuned and implement.

CONCLUSION

In this study, the potential application of the magnetorheological brake system in an automotive vehicle is observed through simulation and experiment. By using the simulated quarter vehicle dynamic model, the capability of the brake system is verified through the sudden braking test in three-speed conditions with two different wheel loads. It is concluded that the PID control used as the brake controller maximised the MRB application in the braking system. The simulation results in this experiment shown that the usage of MRB in the braking system is able to produce the necessary braking torque that is needed to slow down the vehicle to the required speed. In addition, the used of MRB in an actual vehicle braking system is then explore experimentally through a quarter vehicle test rig. By using the same dynamic test in the simulations, the performance characteristics of the MRB hardware are assessed. The results indicated that the MRB actuator produces an overall good response by producing a good similarity in the trend with a less 1-second delay in the time response as compared with the simulations. The delay in time response between experiment and simulations is due to the frictions in the mechanical system. However, if the trend of the model responses is closely similar to the experimental responses with an acceptable level of deviations and errors in magnitude [33], it is considered that the results are acceptable. Therefore, based on the results obtained in this experiment, it is concluded that the usability of MRB in automotive vehicle system is reliable, but an in-depth study should be done before it can be realised.

ACKNOWLEDGEMENT

The authors wish to thank the Ministry of Science, Technology and Innovation, Malaysia, for providing the fund and also to whomever involved in this project.

REFERENCES

[1] Kumar VA, Kalyan S. Active safety braking system. International Journal of Scientific and Research Publications 2013; 3: 1–3.

[2] Milanés V, González C, Naranjo JE, et al. Electro-hydraulic braking system for autonomous vehicles. International Journal of Automotive Technology 2010; 11: 89–95.

[3] Xiong L, Yuan B, Guang X, et al. Analysis and design of dual-motor electro-hydraulic brake system. SAE Technical Paper: 2014-01-2532; 2014.

[4] D'Alfio N, Morgando A, Sorniotti A. Electro-hydraulic brake systems: Design and test through hardware-in-the-loop simulation. Vehicle System Dynamics 2006; 44(1): 378-392.

[5] Miller JI, Cebon D. A high performance pneumatic braking system for heavy vehicles. Vehicle System Dynamics 2010; 48(1): 373-392.

[6] Broadbent HR. Electro-pneumatic brakes. Proceedings of the IEE - Part IA: Electric Railway Traction 1950; 97(1): 250-261(11).

[7] Bauer F, Fleischhacker J. Hardware-in-the-loop simulation of electro-pneumatic brake systems. SAE Technical Paper: 2015-01-2745; 2015.

[8] Farris RJ, Goldfarb M. Design of a multidisc electromechanical brake. IEEE/ASME Transactions on Mechatronics 2011;

16(6): 985-993.
[9] Ahn JK, Jung KH, Kim DH, et al. Analysis of a regenerative braking system for hybrid electric vehicles using an electro-mechanical brake. International Journal of Automotive Technology 2009; 10: 229-234.
[10] Atia MRA, Haggag SA, Kamal AMM. Enhanced electromechanical brake-by-wire system using sliding mode controller. Journal of Dynamic Systems, Measurement, and Control 2016; 138: 41003–41006.
[11] Karakoc K, Park EJ, Suleman A. Design considerations for an automotive magnetorheological brake. Mechatronics 2008; 18: 434–447.
[12] Jo CH, Lee SM, Song HL, et al. Design and control of an upper-wedge-type electronic brake. Proceedings of the Institution of Mechanical Engineers, Part D: Journal of Automobile Engineering 2010; 224(11):1393-1405.
[13] Hills B, Porta PEP, Dwight H. Electromechanically actuated disc brake system. Patent US 5829557, USA 1998.
[14] Farshizadeh E, Steinmann D, Briese H, et al. A concept for an electrohydraulic brake system with adaptive brake pedal feedback. Proceedings of the Institution of Mechanical Engineers, Part D: Journal of Automobile Engineering 2015; 229(6): 708-718.
[15] Jo C, Hwang S, Kim H. Clamping-force control for electromechanical brake. IEEE Transactions on Vehicular Technology 2010; 59(7): 3205-3212.
[16] Kim J, Jo C, Kwon Y, et al. Electro-mechanical brake for front wheel with back-up braking. SAE International Journal of Passenger Cars—Mechanical Systems 2014; 7: 1369–1373.
[17] Kim JG, Kim MJ, Kim JK, et al. Developing of electronic wedge brake with cross wedge. SAE Technical Paper: 2009-01-0856; 2009.
[18] Nam TH, Ahn KK. A new structure of a magnetorheological brake with the waveform boundary of a rotary disk. Smart Materials and Structures 2009; 18: 115029.
[19] Sohn JW, Gang HG, Choi S-B. An experimental study on torque characteristics of magnetorheological brake with modified magnetic core shape. Advances in Mechanical Engineering 2018; 10: 1-8.
[20] Nguyen QH, Choi SB. Optimal design of an automotive magnetorheological brake considering geometric dimensions and zero-field friction heat. Smart Materials and Structures 2010; 19(11): 115024.
[21] George LK, Tamilarasan N, Thirumalini S. Design and analysis of magneto rheological fluid brake for an all terrain vehicle. In: IOP Conference Series: Materials Science and Engineering 2018; 310: 012127.
[22] Shiao Y, Nguyen Q-A. Torque enhancement for a new magnetorheological brake. Procedia Engineering 2014; 76: 12–23.
[23] Qin H, Song A, Zeng X, et al. Design and evaluation of a small-scale multi-drum magnetorheological brake. Journal of Intelligent Material Systems and Structures 2018; 29: 2607–2618.
[24] Semsey Á, Roberts R. Simulation in the Development of the electronic wedge brake. SAE Technical Paper: 2006-01-0298; 2010.
[25] Gombert B, Ho LM, Roberts R, et al. Modeling and control of a single motor electronic wedge brake. SAE Technical Paper Series: 2007-01-0866; 2007
[26] Cheon JS. Brake by wire system configuration and functions using front EWB (electric wedge brake) and rear EMB (electro-mechanical brake) actuators. SAE Technical Paper: 2010-01-1708; 2010.
[27] Kim J-G, Kim M, Chun J, et al. ABS/ESC/EPB control of electronic wedge brake. SAE Technical Paper: 2010-01-0074; 2010.
[28] Zainordin AZ, Abdullah MA, Hudha K. Modelling and validation of magnetorheological brake responses using parametric approach. In: IOP Conference Series: Materials Science and Engineering. 2013; 50: 012038.
[29] Zainordin AZ, Abdullah MA, Hudha K. Experimental evaluations on braking responses of magnetorheological brake. International Journal of Mining, Metallurgy and Mechanical Engineering 2013; 1: 1–5.
[30] Zainordin AZ, Hudha K, Jamaluddin H, et al. Design and characterisation of magnetorheological brake system. International Journal of Engineering Systems Modelling and Simulation 2015; 7: 62–70.
[31] Zainordin AZ bin, Hudha K, Jamaluddin H, et al. Design and characterisation of magnetorheological brake system. International Journal of Engineering Systems Modelling and Simulation 2015; 7(1): 62-70.
[32] Xu J, Li Y, Xu L, et al. A multi-mode rehabilitation robot with magnetorheological actuators based on human motion intention estimation. IEEE Transactions on Neural Systems and Rehabilitation Engineering 2019; 27(10): 2216-2228.
[33] Hudha K. Non-parametric modelling and modified hybrid skyhook groundhook control of magnetorheological dampers for automotive suspension system. PhD thesis, Universiti Teknologi Malaysia, Malaysia, 2005.
[34] Rykiel EJ. Testing ecological models: the meaning of validation. Ecological Modelling 1996; 90: 229–244.